

Experimental characterization of burning
velocities of premixed methane-air and hydrogen-
air mixtures in a constant volume combustion
bomb at moderate pressure and temperature

Miriam Reyes^{1}, Francisco V. Tinaut¹, Alfonso Horrillo², Alvaro Lafuente²*

1 Department of Energy and Fluid-Mechanics Engineering, University of Valladolid,

Paseo del Cauce, 59, 47011, Valladolid – SPAIN

2 CIDAUT Foundation, Parque Tecnológico de Boecillo p. 209, E-47151 Boecillo-

Valladolid, Spain

* miriam.reyes@uva.es

KEYWORDS. Laminar burning velocity, methane, hydrogen, constant volume combustion
bomb, two-zone combustion analysis model,

ABSTRACT

Burning velocities of methane-air and hydrogen-air mixtures are investigated in a spherical constant volume combustion bomb varying the initial conditions of pressure, temperature and fuel/air equivalence ratios. Present work describes a method to determine burning velocities based on the use of a combustion bomb, in which the temporal pressure evolution is registered. A two-zone combustion model is used to analyse the experimental pressure trace and compute the thermodynamic variables that cannot be directly measured, with the mass burning rate and the associated burning velocity as the model results. The main interest of using a constant volume combustion bomb is the possibility of reaching high values of pressure and temperature, similar to the case of the combustion process in reciprocating internal combustion engines. The values obtained for the burning velocity are presented in the form of correlations as power laws of pressure and temperature, with exponents that depend on the equivalence ratio. A particular attention is paid to the validation of the burning velocity of methane-air at ambient values (300 K and 0.1 MPa), for which many experimental results are reported in literature. The first set of results include the combustion of methane-air mixtures at an initial temperature of 300 K, initial pressures of 0.05, 0.1 and 0.15 MPa, and equivalence ratios of 0.7-1.2. The ensemble of obtained burning velocities is in the range of laminar flame regime (excluding the cellular regime), covering the initial range of engine conditions (320-480 K, 0.1-0.7 MPa). These results are in a good agreement with data obtained by other authors. A second set of results refers to stoichiometric hydrogen-air mixtures at temperatures of 320 to 650 K and pressures of 0.1 to 1.6 MPa. Due to the particular characteristics of hydrogen, since it is almost impossible to have purely laminar combustion at stoichiometry when the pressure grows, the obtained values of the burning velocities are in the cellular regime. A discussion of the comparison of the present results with other authors' results is included, with considerations about the experimental and numerical approaches.

1. Introduction

The burning velocity of laminar premixed flames has been the subject of extensive experimental and theoretical research for a long time. It is a concept of practical importance in the analysis, design and performance of reciprocating internal combustion engines (RICE), because it has an effect on the burn rate in the engine, its efficiency and emissions [1]. Burning velocities are also important for developing and testing combustion models and validating complex kinetic mechanisms. Obtaining the laminar burning velocity of fuel mixtures can be accomplished with several methods, usually by combining experimental techniques (pressure register, image record) and analyses of measured data (thermodynamic models, asymptotic analysis of instabilities, account for stretch effects).

Obtaining the correlations of laminar burning velocity for combustible gas mixtures as functions of pressure, temperature and air fuel ratio is of a great importance for evaluating the effect of fuels in spark ignition engines (SIE).

In a gaseous, premixed and homogeneous fuel mixture, with a given composition, temperature and pressure, the laminar burning velocity is defined as the propagation velocity (related to the unburned mixture) of a one-dimensional, adiabatic, flat and stable flame front [2]. The laminar burning velocity of that ideal one-dimensional flame only depends on the composition, temperature and pressure of the mixture. It is an important physic-chemical

property of the fuel mixture, as it provides a measure of its diffusivity, reactivity and exothermicity.

Kuo [3] explains and classifies different theories used to study the ideal one-dimensional flame as a function of the effect which is considered dominant in the combustion. That is, thermal theories, where heat diffusion is assumed to be the phenomenon which controls the combustion, diffusive theories if the mass diffusion is the controlling process, and global theories, which consider both the effects of mass and heat diffusion on the process. Asymptotic analyses can be found in the works of Clavin [4] and Williams [5]. One of the purposes of these theories is to find an analytical expression for the laminar burning velocity of a mixture as a function of different physico-chemical properties of that mixture.

In actual experimental situations, it is impossible to reach an ideal flame (one dimensional, plane, adiabatic and stable flame), so that, the results of the laminar burning velocity measurements given by the different methods correspond to the burning velocity of the particular flame conditions that can be established in each case. The more similar conditions of the experimental flame to the conditions of the ideal one-dimensional flame, the closer the values of the laminar burning velocity will be to those of an ideal one-dimensional flame. In addition, there is not a standardized method to measure the laminar burning velocity, so that, the results published show a notable dispersion with the values obtained by other authors [6].

In a standard classification, the experimental methods for the determination of the laminar burning velocity are divided into two classes: In some of them the flame is kept stationary while in others the flame front moves relatively to a fixed reference system. In the first class, *stationary flame methods*, which rely on measurements of the flow structure of stabilized flames, divergent flux flames (counterflow [7] and stagnation flame [8],[9]) and burners [2],[10],[11],[12] are included. In the second class, *non-stationary flame methods*, the fuel mixture is initially steady; after the ignition process, the flame advances with a certain velocity with respect to the fixed reference system. The tube method [13],[14] and combustion bomb methods [15],[16] are included in this second class.

An additional classification would be based on the pressure and temperature conditions reached by each method. In the tube and stationary flame methods, it is more usual to find results at ambient conditions or slightly higher conditions. On the contrary, constant volume combustion bombs allow obtaining the values of burning velocity for higher values of pressure and temperature, even reaching what it is known as engine-like conditions (up to about 5 MPa and 900 K).

Based on a combustion bomb test rig, there are different methods to directly or indirectly track the deflagration of a fuel mixture inside the bomb, and from that information, the laminar burning velocity can be measured or calculated from other variables. The main advantage of these methods is that, with a robust design of the combustion bomb, they are convenient to determine the burning velocity at elevated pressure and temperature conditions. The method of the combustion bomb has two versions[17],[18],[19]: Registration of pressure as a function of time[20],[21],[22],[23], and image recording of the flame front[24],[25]. With the first method the burning velocity is obtained from the temporal evolution of pressure during the combustion process by means of the application of a two-zone analysis model. With the second method, the burning velocity is obtained from the evolution of flame front radius versus the time during the first stages of the combustion, when the pressure (and the temperature) of the fresh mixture has not almost been increased and thus can be considered constant. Additional provisions have

to be made to distinguish between combustion velocity and flame front velocity, due to burned gas expansion.

In both methods, once the mixture is prepared inside the combustion chamber, it is ignited. Usually, only one point of ignition is used, located at the geometrical centre of the chamber of combustion. However, there are several methods that use the simultaneous ignition in two different points of the combustion chamber.

In the cases with a central, one-point ignition, a flame front is generated which, neglecting the floatability effects, can be considered spherical and centred at the ignition point. The flame front moves outwards and meanwhile, the expansion of the burned gas increases pressure and temperature due to the adiabatic compression of the unburned gas. For that reason, conditions of pressure and temperature of the fresh (unburned) mixture which is burning inside the bomb change during the combustion process. The propagation speed of the flame front in the confined volume is not only due to the burning velocity of the combustion process on the unburned mixture. The mixture inside the bomb is static before the combustion process, but once it is ignited, the lower density of the burned gases (due to their higher temperature) causes an expansion and the simultaneous compression of the unburned mass during the combustion. Therefore, the flame front propagation speed S_f , is the addition of the gas velocity due to the flame expansion, u_g , and the burning velocity C_c . More detailed descriptions of the gases movement can be found in Dahoe [15] and Gillespie et. al. [25].

The increase of unburned mixture temperature during the combustion process causes also an increase of the flame front velocity from the bomb centre to the wall. In some works [26] the dependence of the burning velocity with the curvature of the flame front is analysed and the existence of a smooth laminar flame front is even questioned in the case of high pressures and temperatures, due to the appearance of cellularity.

Many authors have investigated the burning velocity of hydrocarbon-air mixtures, including methane-air mixtures ([27], [28], [29], [18], [23], [30], [31], [32], [33], [30] between others) and other hydrocarbons as butane [34]; and hydrogen-air burning velocity ([35], [21], [36], [37], [38], [39], [40], [41], [42], [43], [44] and [45]) in different devices. Also many authors study the influence of adding hydrogen to methane blends. Hu et. al. [46] developed an study of the effect of hydrogen addition on the laminar burning velocity of methane and flame structure for ambient conditions. Huang et al. [47] studied the laminar flame characteristics of natural gas-hydrogen-air flames and the influence of stretch rate on flame. Hu et al. [41] carried out an experimental and numerical study on the lean methane-hydrogen-air flames at elevated pressures and temperatures. Bradley et al. [48] developed blending laws for laminar burning velocity and Markstein length for mixtures of CH_4 /air and H_2 /air. Changwei et al. [49] obtained values of methane/hydrogen/air burning velocities from simulations under various conditions by PREMIX code by using different mechanisms, and their results are compared with literature. Nilsson et al. [50] studied the effect of hydrogen addition on the laminar burning velocities of methane and blends of methane with ethane and propane. Burning velocities of methane-air mixtures will be studied in detail in section 4.1, and the corresponding hydrogen burning velocities will be extensively revised in section 4.2.

The method used in the present work to determine the burning velocity of fuel mixtures uses a constant volume combustion bomb, where pressure is registered during the combustion process. The pressure register and the rest of operational variables (initial temperature, mass of gases, mixture composition and equivalence ratio) are the inputs to a two zone diagnostic model, with temperature dependent thermodynamic properties and heat losses, used to evaluate

the burning rate and obtain the burning velocity. This method, was chosen because it has two fundamental advantages. First, it allows obtaining values of the burning velocity at pressures and temperatures that are moderate (up to 1.6 MPa and 650 K), in an attempt to approximate to engine-like conditions. Second, one single test allows obtaining the values of the laminar burning velocity for all the values of p-T couples reached during the combustion process. Third, the careful filling process allows to obtain repetitiveness in the results.

In addition to presenting the general methodology, results of burning velocity of methane-air and hydrogen-air mixtures for different equivalence ratios and initial conditions of pressure and temperature are shown. To demonstrate the validity of the method these values are compared with the results obtained by other authors.

2. Experimental setup: Constant Volume Combustion Bomb

The experimental set up used by the authors consists of a test facility designed for the study and characterization of the combustion process of gaseous and liquid fuels. The main components are a constant volume combustion bomb (CVCB), an acquisition system to register information about the development of the combustion, and supply lines for the introduction of fuels. Gaseous mixtures are typically formed by CO, CO₂, H₂, N₂, CH₄ and N₂, which are stored in pressurized tanks, and synthetic or compressed outdoor air. The tanks of CO, H₂ and CH₄ are located in a safety closet with ventilation because of their toxicity or flammability. All the gas supply lines join in the regulation panel by means of a set of pipes and valves, see Figure 1. This test rig has been also used for combustion of liquid fuels, but this requires previously their evaporation in order to guarantee a homogeneous fuel air mixture prior to combustion start [16].

In Figure 1, a schematics of the experimental setup can be seen, where the CVCB is a stainless steel spherical cavity of 200 mm diameter, with pressure and temperature transducers and two optical access holes. The CVCB has been designed to withstand pressures up to 40 MPa and temperatures up to 1073 K during the development of the combustion. There are two electrodes inside the CVCB between which the spark is discharged to start the combustion at the geometric centre of the sphere.

At the beginning of each combustion process, initial conditions of pressure, temperature and fuel/air ratio have to be set up. Mixtures of fuel and air are introduced in the CVCB at the desired initial conditions of pressure and temperatures. Once the combustion is initiated, a spherical flame front propagates inside the CVCB compressing and burning the fresh mixture. During the combustion process development, the evolution of the pressure is registered by a piezoelectric transducer Kistler 7063 type (maximum calibration error 0.06%). This transducer is cooled to protect it from high temperatures. This sensor was connected to a KISTLER 5018A1000 charge amplifier (maximum calibration error of 0.3%). The output signal of the charge amplifier was recorded on a Yokogawa DL750 Scopecorder (16 bits AD converter). The estimated error of the pressure acquisition is 0.36% over the measuring range. The acquisition system allows obtaining up to 30,000 data per second.

An example of pressure registers as a function of time can be seen in Figure 2, for stoichiometric methane/air equivalence ratio and for the three values of initial pressure tested.

Time zero corresponds to spark ignition. Pressure increases as combustion develops, with the spherical flame front growing from the bomb centre, reaching a maximum when all the mixture is burned and the flame front reaches the bomb wall, and then decreasing due to heat transfer to bomb wall. The pressure increase is related to the mass fraction burned and then to the burning velocity. It can be observed for instance that, as the initial pressure increases, the pressure during the combustion is also higher and the duration of the combustion is longer, providing the first evidence of the inverse relation between the burning velocity and the pressure for this mixture of methane and air. However it is necessary a two-zone model to be able to compute the burning velocity from the pressure, as described in the next section.

Additional details of the experimental facility and on the complementary use of the radiation of OH and CH radicals for the analysis of the rate of heat release can be seen in Tinaut et al. [51].

3. Combustion analysis model

The burning velocity is determined by a thermodynamic analysis of the pressure data registered during the combustion process in the constant volume combustion bomb. The main input of the two-zone combustion analysis model is the temporal evolution of the pressure registered during the combustion, in addition to the initial values of the fuel composition and mass of the gaseous mixture.

This model considers the division of the combustion chamber in two different zones: Burned (denoted with a b subscript) and unburned (denoted with a ub subscript, see Fig. 3). Conservation equations and ideal gas equations are applied in each zone, [16, 52-54]. During combustion, the unburned zone converts into burned zone, which starts at the geometric centre of the sphere from the ignition caused by a spark plug. Thus, the burned zone grows spherically in a way concentric with the vessel wall. Among other variables, the outputs of this model are the temperatures of the unburned mixture and burned zone, the burned mass fraction, the flame front surface and the burning velocity [16].

The burning velocity C_c is calculated from the mass burning rate \dot{m}_b , the unburned mixture density ρ_{ub} and the flame front surface A_f , according to the following expression:

$$C_c = \frac{\dot{m}_b}{\rho_{ub} A_f} \quad (1)$$

An example of results of the two-zone model is presented in Figure 4, where the experimental pressure is plotted versus the combustion time, together with some of the most important model results: the mass fraction burned (MFB), the flame radius and the burning velocity. A plot such as the one in Figure 4 provides a value of the burning velocity $C_c = C_c(p, T_{ub})$ for each couple pressure-temperature of the unburned mixture (temperature is not plotted in the figure, but it is also calculated by the model). A value of mass fraction burned equal to 0.05 is depicted as the initial validity point for burning velocity (after oscillations due to spark energy effect and numerical mechanism). Another final validity limit is set to exclude points affected by cellularity (characterized by a bump in the velocity plot).

To assure that the obtained results of burning velocity $C_c(p, T_{ub})$ are independent of the initial conditions of the experiment, a methodology is used to overlap combustion speeds corresponding to the same pressure and temperature, but obtained in different combustion processes starting from different initial conditions.

Overlapping curves allow comparing the burning velocity for flame fronts with different radius but similar conditions of pressure and temperature. Figure 5 shows the pressure and burning velocity of two combustion processes (a and b) whose initial conditions $(T_{i,a}, p_{i,a})$ and $(T_{i,b}, p_{i,b})$ have been chosen to show a good overlap of ranges of validity of burning velocity. It can be seen that there is a common range in which the burning velocity of both experiments have a common or overlapping range. This overlapping range covers from the start of validity range of experiment b (the one with higher initial conditions) to the end of validity range of experiment a (the one with lower initial conditions).

In Figure 6, the overlapping curves of 12 different combustion processes of stoichiometric methane/air mixtures are represented. The burning velocity and pressure are plotted in this figure versus the unburned mixture temperature. The initial conditions of the first experiment (at the top left hand side of the figure) are 298 K and 0.1 MPa. The initial temperature for the following experiments has been incremented each in 25 K. The initial pressure of each consecutive experiment is the one corresponding with the p - T_{ub} line of the evolution of the previous experiment. The same colour has been used to plot the lines of burning velocity and pressure in each experimental condition. As can be seen, there is a homogeneous trend of the burning velocity, with values that overlap for the corresponding same values of pressure and temperature, independently of the flame front position. This confirms the repeatability of the process and also that the burning velocity obtained for a given mixture is only function of the pressure and temperature, while it is independent of the flame front radius.

An additional issue is if the burning velocity during the combustion process in the bomb can be considered laminar. Since the mixture is initially quiescent, there is no initial turbulent effect due to flow. Then the combustion process is laminar during the main part of the process, with the exceptions of the beginning and the last part of the combustion, due to two phenomena that affect the burning velocity: The stretch and the apparition of cellularity in the flame.

As indicated previously, there are some parts of the burning velocity graphs that are discarded of the results obtained in each experimental combustion process. These parts include some of initial points (due to spark effects on combustion onset, numerical oscillations and stretch effects) and some of final points (due mainly to cellularity effects). The identification of these effects defines the validity range of a given experiment, as shown in Figure 5. Under certain conditions, a cellular combustion regime is established with a distorted flame front that results in an apparent burning velocity bigger than the laminar one, if both velocities are referred to a smooth flame front (e.g. plane or, as in the present case, spherical). Hu et al. [55] explains this process because the formation of cells is a consequence of diffusional thermal instability, which results from the competing effects of heat conduction from the flame and reactant diffusion toward the flame. It is well known that even for moderate pressure a cellular regime is established for methane. In Figure 6, it can be seen that for all pressures higher than 0.7 MPa (corresponding to unburned mixture temperatures bigger than 500 K) the apparent velocity is higher than the combustion velocity obtained as an extrapolation of the purely laminar regime (thick black line). This situation has to be accounted for when analysing experimental data, in order to distinguish between the laminar and cellular regime. This can be done fairly easily for methane, but it is much more difficult in other cases, such as hydrogen.

In addition to the possible apparition of cellularity, the last part of the combustion process has also to be discarded because the flame front approaches the wall and this interferes on the free development of the flame. The temperature of unburned gases can also be affected locally by heat transmission, and then the hypothesis of adiabatic compression for the unburned gas temperature calculation ceases to be satisfied. Also buoyancy effects may appear when the volume of the burned zone is high [16], with the flame front radius close to the combustion bomb radius (100 mm).

4. Results of burning velocity of methane-air and hydrogen-air mixtures

Results of the burning velocity of methane-air and hydrogen-air mixtures are presented for different equivalence ratios and a broad range of initial conditions of pressure and temperature. The results obtained are presented in two parts. First, the validation of the methodology is assured by comparing the results of methane burning velocity with other authors' results for both ambient conditions (300 K, 1 MPa) and moderate conditions (up to 480 K and 0.7 MPa, range of laminar flame). In a second place, results obtained with hydrogen-air mixtures are also presented and compared with other published results.

4.1. Determination of burning velocity of methane-air mixtures

Methane has some characteristics which make it more adequate than other gaseous fuels to be chosen as a reference fuel to compare results and validate the methodology. The burning velocity of the stoichiometric mixture of methane-air at ambient conditions is relatively high (about 0.36 m/s), which means that floatability effects due to changes in density are less important (i.e. a relatively small value of the Froude number) and can be neglected.

Laminar burning velocity of methane at ambient conditions

While there are many published values of the burning velocity of methane-air mixtures under stoichiometric conditions at ambient conditions of pressure and temperature, the dispersion of the results is important. For example, a revision made by Andrews and Bradley [56] of the values of the burning velocity in mixtures of methane and air published until the year 1972, for the equivalence ratio corresponding with the maximum velocity, showed a dispersion between 0.32 m/s and 0.50 m/s.

A more recent revision made by Bosschaart and de Goey [29] compiles results published until the year 2002 obtained with diverse experimental techniques. From those results they conclude that the value of the burning velocity of a stoichiometric mixture of methane and air at ambient conditions is 0.36 ± 0.01 m/s.

Table 1 summarises some published works relative to methane-air laminar combustion velocity obtained by experimental techniques, including author, year, method, pressure and temperature.

Figure 7 shows the values of laminar combustion velocity of methane-air mixtures at close-to-ambient conditions (300K, 0.1 MPa) for different equivalence ratios obtained by the authors listed in Table 1, together with the results of the methodology presented in this work (black dots)

As can be seen, the authors' values are systematically in the midrange of the other researchers' values, giving confidence that the methodology developed in this work for the determination of the laminar burning velocity is valid. In particular, the result of methane burning velocity for 300K, 0.1 MPa, and $\Phi=1.0$ is 0.366 m/s. This value is inside the above said interval of confidence proposed by Bosschaart and de Goey [29] of 0.35-0.37.

Laminar burning velocity of methane at moderate conditions

Once the methodology has been validated, twenty-one experiments (three initial pressures combined with seven equivalence ratios) of methane-air mixtures have been carried out. The initial temperature is kept to 300 K, while three initial values of pressure (0.05, 0.10 and 0.15 MPa) and seven values of equivalence ratio (0.7, 0.8, 0.9, 1.0, 1.05, 1.15 and 1.2) are considered.

Figure 8 shows the results of pressure and combustion velocity for the twenty-one combustion experiments. In each graph, results of pressure and burning velocity for the experiments are represented versus the unburned temperature, with three initial pressures made for each methane/air equivalence ratio. Pressure values correspond to the always increasing lines (with a scale on the right axis) while burning velocity values are represented by the lines with a zero initial value, an almost linear section and a value reducing to zero when combustion ends (with a scale on the left axis). In all graphs, lines corresponding to the same initial pressure are represented in the same colour: green for 0.05 MPa, red for 0.10 MPa and blue for 0.15 MPa. Notice that, in spite of the fact that the initial values of pressure are relatively low (0.05, 0.10 and 0.15 MPa), pressure grows during combustion up to values of the order of 0.4 to 1.3 MPa, while unburned mixture temperature can be up to 530 K (depending on the initial pressure and equivalence ratio).

The laminar range of validity of the burning velocity in the linear section is highlighted with a thick trace in its respective colour. The selection of each range of validity has been made due in order to exclude the cellular regime data. The valid points are used to obtain the laminar burning velocity correlations as a function of pressure and temperature.

Some general trends of the burning velocity can be identified. In general, burning velocity of methane-air mixtures grows with temperature but decreases with pressure. Apart from that, for values of pressure above of about 0.60 MPa, the apparition of cellularity creates an appreciable increment in the apparent burning velocity, although not for all values of equivalence ratio (e.g. not present for 0.7 equivalence ratio).

All data of the (purely) laminar burning velocity belonging to the range of validity have been adjusted to a power law correlation, similar to the one proposed by Metghalchi-Keck [22], as given by Eq. 2 (with $T_{ub0} = 300$ K and $p_0 = 0.1$ MPa), where α , β and C_{c0} are the resulting parameters of the adjustment for a certain gas mixture (i.e. composition and equivalence ratio).

$$C_c (m/s) = C_{c0} \cdot \left(\frac{T_{ub}(K)}{T_{ub0}} \right)^\alpha \cdot \left(\frac{p(Mpa)}{p_0} \right)^\beta \quad (2)$$

In Table 2 the values of the coefficients C_{c0} , α and β of Eq. 2 are shown for the corresponding methane-air equivalence ratios of the mixtures, from the results shown in Figure 7, covering pressures of 0.1-0.7 MPa and temperatures of 320-480 K. These ranges are conservative, since for instance for stoichiometric conditions the correlation includes data up to 0.9 MPa. Table 2 also includes the values of the correlation coefficient R^2 and the standard error of estimation.

In the last row of Table 2 the expressions of coefficients C_{c0} , α and β of Eq. 2 are shown as functions of the methane/air equivalence ratio, valid for equivalence ratios ranging from 0.7 to 1.2, and the same ranges of temperature and pressures.

One detail to be pointed out is that the value of C_{c0} appearing in Table 2 does not provide the best value of the laminar velocity at the reference conditions (300 K and 0.1 MPa). This value is obtained from the specific experiments reported in Figure 7 (i.e. 0.366 m/s at stoichiometry, and similarly for other equivalence ratios). The reason for these discrepancies is that the coefficient C_{c0} of the power law correlation of Eq. 2 appearing in each row of Table 2 are obtained as the best regression fit of the experimental results over wide ranges of pressure and temperature (Figure 8) higher than the ambient ones. Then, the particularisation of the general regression at the origin is affected by all other results.

Comparison with other authors' results at moderate conditions

The present results of burning velocity of methane-air (summarised in the form of Eq. 2 with the coefficients of Table 2) are now compared at moderate pressure and temperatures with the results obtained by other authors: Iijima and Takeno[21], Gu et al.[18]; and Stone et al.[31].

The correlation obtained by Iijima and Takeno[21] was obtained from experiments in a constant volume combustion bomb with pressure register. It offers burning velocity values valid up to high pressure, although in their work the authors do not mention if the correlation is for a purely laminar flame or if it includes cellular results. The range of validity of this correlation is: $0.8 < \Phi < 1.3$; $0.5 < p \text{ (atm)} < 30$ and $291 < T_{ub} \text{ (K)} < 500$.

The correlation proposed by Stone et al. [31] was obtained by a method similar to the one used in this work, but with measurements performed inside a combustion bomb during a free fall, to avoid the possible deformations of the spherical geometry as a consequence of the floatability phenomenon. The range of validity of this correlation is: $0.6 < \Phi < 1.4$; $0.05 < p \text{ (MPa)} < 1.04$ and $300 < T_{ub} \text{ (K)} < 450$.

A more recent correlation proposed by Gu et al.[18] is also obtained in a constant volume combustion bomb, but with a methodology which allows visualizing the flame front and observing its distortions during the combustion; thus the authors can assure that this correlation is for a laminar flame front, for a range of validity: $0.5 < p \text{ (bar)} < 10$ and $300 < T_{ub} \text{ (K)} < 400$.

The ranges of validity of these four correlations are represented in a thermal map in Figure 9 with different colours. The full range of the experimental results of the present work is shown

in black, while the reduced range of purely laminar conditions in the absence of cellularity appears in black with broken lines.

In Figure 10 the results obtained by the burning velocity expressions of the three other authors are compared with the present experimental data (black line) and the associated correlation (Eq. 2, fuchsia). The values are computed as a function of both the unburned mixture temperature and the associated compression pressures (grey line) that would occur in the combustion chamber of an engine, starting in each case at 0.15 MPa (top), 0.10 MPa (middle) and 0.05 MPa (bottom).

The results of the correlations of Gu et al.[18] (in blue) and Stone et al.[31] (in green) provide similar values, especially at lean conditions and low and intermediate pressures, with a certain discrepancy at higher pressures. At rich conditions, both results almost coincide at intermediate pressures, but the absolute values invert their trends from low to high pressures.

However the correlation of Iijima and Takeno [21] (in red) provides values that are systematically higher than the results of the rest, except at stoichiometry and close to ambient conditions. This can be due to the fact that in their work Iijima and Takeno [21] included data obtained at pressures ranging from 1 to 3 MPa, a pressure range much higher than that of the rest of correlations. In addition their data were obtained without making distinction of the possible apparition of a cellular flame front. Stone et al.[31], with a method similar to the one used in this work, and with data obtained at pressures up to 1 MPa, indicated that they did not find evidences of the existence of a cellular flame front. However, Rahim [59], using a constant volume combustion bomb of the same size than the used by Stone et al.[31] (150 mm diameter), also shows pictures of cellular flame fronts above 0.6 MPa pressure. In the present work the authors have also found evidences of cellular flame front for pressures higher than 0.6 MPa for some mixtures. In Figure 10, the burning velocities for conditions at which a cellular regime may appear are not plotted (i.e., lean and stoichiometric mixtures at high pressures).

In the ranges of pressure and temperature common to the four correlations, the correlation obtained in this work provides values similar to those of the correlations of Stone et al.[31] and Gu et al.[18] for lean mixtures and all values of pressure. The agreement is also reasonable for stoichiometric mixtures at higher pressures, and somewhat worse at lower pressures, for which the results are more similar to those of Ijima. For rich mixtures, the authors' correlation provides values very similar to the ones of Gu et al. (blue) at lower pressures and to Stone et al. (green) at higher pressures.

4.2. Burning velocity of hydrogen-air mixtures

Once the methodology for the determination of the burning velocity in the CVCB has been validated, we proceed to present results obtained for hydrogen-air mixtures at different initial conditions.

Experiments and proposed correlation for hydrogen-air mixtures

Some experiments have been developed in the CVCB with the objective of obtaining the burning velocity correlation of the stoichiometric hydrogen-air mixture for moderate conditions of pressure and temperature. In Figure 11 it can be seen an example of the evolution

of combustion pressure vs. time of stoichiometric mixtures of hydrogen-air with different initial pressures and temperatures.

In general, burning velocities of hydrogen-air mixtures are much higher than the values of the methane-air mixtures. For example, the burning velocity of a hydrogen-air mixture at stoichiometric mixtures and ambient conditions is 2.47 m/s, about seven times higher than the value for a similar methane-air mixture (0.366 m/s).

Furthermore, it is important to mention two additional characteristics of the hydrogen-air experiments, different from the methane-air experiments. First, the flame front of the hydrogen-air mixtures has more tendencies to present instabilities, especially in lean fuel/air equivalence ratios. This unstable behaviour promotes the apparition of cellular flame front in the experiments developed in the CVCB. Second, it is very usual to find strong oscillations in the pressure register obtained during combustion of hydrogen. Dahoe [15] also found these instabilities in experiments with hydrogen mixtures made in constant volume combustion bombs. These instabilities can be explained as the induced velocity in the burned mixture as a consequence of the expansion of the layer near the wall when they burned. Bradley et al. [60] considered that they are acoustic oscillations which are produced, mainly, in mixtures with low Markstein numbers, and which interact with the flame front inducing the early apparition of a cellular flame front.

The results of the burning velocity and the associated pressure of seven experiments of hydrogen-air mixtures at stoichiometric conditions are represented in Figure 12 versus the unburned temperature. To smooth down part of the oscillations of the experimental pressure, a low band filter of 4 kHz has been used. The initial conditions of the first experiment were 298 K and 1 bar. Each one of the following experiments had an initial temperature increased in 25 K above the previous one, while the initial pressure was the necessary to reach that temperature by compression. In this figure it is possible to see the perfect overlapping of the lines of pressure and burning velocity of the seven experiments.

The good overlapping of the lines shows the internal coherence of experimental data, because the values of the burning velocity are independent of the flame front size. On the contrary they are only dependent on the pressure and unburned mixture temperature. In the overlapping plots of methane a bump in the burning velocity could be seen (characteristic of the transition to cellular regime, Fig. 6), but in the hydrogen case it is not possible to detect that bump. As the hydrogen-air mixture presents more tendencies to instabilities and pressure triggers the cellular flame apparition, the change from a laminar flame front appears much before than in the methane case. In fact, it happens that the flame front of the hydrogen-air mixtures is cellular in the full range of the present experiments. More authors [61] support this assumption by direct visualization of the flame front, since they carry out experiments with hydrogen-air mixtures in the same range of pressure and temperature in a combustion bomb with optical access.

Values of the burning velocity, in stoichiometric conditions, have been adjusted to a correlation similar to the case of methane, which results in the following Eq. 3, with $T_{ub0} = 300$ K and $p_0 = 0.1$ MPa, a correlation coefficient $R^2 = 0.967$ and a standard error of estimation of 0.15 m/s:

$$Cc(m/s) = 2.47 \left(\frac{T_{ub}(K)}{T_{ub0}} \right)^{1.19} \left(\frac{p(MPa)}{p_0} \right)^{0.26} \quad (3)$$

The range of validity of the correlation is 320-650 K and 0.1-1.6 MPa. However it should be noted that, since the experimental data cover points for which pressure and temperature grow simultaneously, the correlation provides reliable values of flame velocity when both variables have the same trend. On the contrary, good results are not assured for combinations of low pressure-high temperature or the reverse.

Figure 13 shows how the correlation fits the results of the experimental tests for different values of unburned mixture temperature (and the related pressure corresponding to the compression that provides that temperature).

In the following a more complete comparison between the present results and the analytical expressions obtained by other authors is done.

Brief summary of published hydrogen combustion velocity data

Several references of hydrogen combustion velocity published by other authors are now considered, presented in a chronological order. Due to the interest of using hydrogen as fuel, in ICE it is important to obtain accurate data of the burning velocity at different conditions of pressure and temperature, and mixed with residual gases. Some of the works presented have an experimental basis, while other develop models (multizone thermodynamic or computational fluid dynamics models) to obtain burning velocity data in different conditions, next to ICE.

Milton and Keck [35] obtained a correlation from registering pressure in a constant volume bomb valid for a stoichiometric mixture in the range of pressure of 0.5-25 atm and temperature of 300-500 K. A thermodynamic analysis was used to calculate the laminar burning velocity from a pressure time history of the combustion process. Their results are presented as a correlation that is formally similar to that of the authors (Eq. 4), with similar values of the exponents, but a slightly different reference velocity:

$$C_c \text{ (m/s)} = 2.17 \left(\frac{T_{ub} \text{ (K)}}{298} \right)^{1.26} \left(\frac{p \text{ (MPa)}}{0.101325} \right)^{0.26} \quad (4)$$

Ijima and Takeno [21] obtained a correlation from the pressure in a constant volume combustion bomb for pressures of 0.5-25 atm, temperatures of 291-500 K and equivalence ratios of 0.5-4. The dynamic pressure was used to make an immediate calculation of the instantaneous burning velocity.

Formally their correlation has two factors: a power of unburned temperature factor, with an exponent that depends on the equivalence ratio, and a logarithm of pressure factor, with a coefficient function of the equivalence ratio. The reference velocity also depends on the equivalence ratio, with the maximum velocity achieved for an equivalence ratio of 1.7 at ambient conditions.

Verhelst [36] developed a correlation for hydrogen flames based on the data most relevant for engine like conditions, built from data of burning velocities obtained in a CVCB at a radius of 10 mm with photographic observation, and based on stretched burning velocities.

Verhelst and Sierens [37] developed a simulation program to calculate the pressure and temperature development in hydrogen engines. A laminar burning velocity correlation developed previously by the authors [36] is combined with some turbulent burning velocity models in a quasi-dimensional two-zone combustion model. Later, simulation results are compared with experimental cylinder pressure data recorded on a single cylinder hydrogen engine.

Knop et al. [38] modelled the combustion of hydrogen with a 3D CFD code (Extended Coherent Flame Model, ECFM) modified to take into account the high laminar burning velocity of hydrogen and its characteristics. They used the correlation for the burning velocity of hydrogen proposed by Verhelst and Sierens [37].

D'Errico et al. [39] developed a numerical and experimental investigation on a single-cylinder hydrogen spark ignition engine. They simulated a hydrogen fuelled spark ignition engine with a multi zone combustion model to predict the burning rate of hydrogen/air mixtures.

Verhelst et al. [40] presented a more complete correlation for the burning velocity of hydrogen/air mixtures aimed to be applied in the internal combustion engines field. The correlation takes again the form of a power law of both unburned temperature (with a constant exponent of value 1.232) and pressure (with a variable exponent depending on the equivalence ratio, with two ranges). The reference velocity depends on the equivalence ratio. An additional factor is included to account for the presence of residual gases (i.e. products of a previous combustion cycle, very important in the case of internal combustion engines). This factor includes again the effect of equivalence ratio.

Hu et al. [41] conducted an experimental and numerical study on hydrogen–air flames at elevated pressures. They obtained a correlation of laminar burning velocity in a constant volume combustion chamber using high-speed Schlieren photography and they validated it with the Chemkin code. Gerke et al. [42] derived burning velocities of premixed hydrogen/air flames at engine-relevant conditions using a single-cylinder compression machine with optical access using OH-chemiluminescence and in-cylinder pressure analysis. They obtained a correlation for the burning velocity relevant for internal combustion engines, ranging from 350 K to 700 K, 5 bar to 45 bar and an air/fuel equivalence ratio covering the range between 0.4 and 2.8. Verhelst et al. [43] developed a computational correlation for the laminar burning velocity of hydrogen (with and without residual gases) for use in a hydrogen spark ignition engine simulation. Gottgens et al. [44] in an early work supplied analytical expressions for the burning velocity of lean hydrogen using numerical computations based on a detailed kinetic mechanism. Bougrine et al. [45] also made a numerical approach to evaluate premixed flame properties of methane and hydrogen mixtures by using complex chemistry. They obtained laminar flame speeds and thicknesses correlations, which were in a very good agreement with previous results.

Comparison of hydrogen combustion velocity with other authors' correlations

The correlations proposed by the previous authors plus the one obtained in this work (given by Eq. 3) are presented as lines of Figure 14 for stoichiometric conditions. Before proceeding to the discussion comparing the published results, it is important to point out that the values of

hydrogen combustion velocity plotted in Figure 14 include the simultaneous effect of both temperature and pressure, since the pressure at each temperature is the one that would provide it due to adiabatic compression (i.e. $p \propto (T_{ub})^{\gamma/(\gamma-1)}$). The comparison is then relevant in terms of engine behaviour, since in engines, both variables grow simultaneously.

As can be seen from the comparison of the results of several authors, there is a big dispersion between them. One reason for that is the difficulty to achieve experimentally measured data for the laminar burning velocity of hydrogen mixtures at engine conditions. In addition, the dispersion between absolute values also comes from the fact that different experimental techniques provide different estimations of flame velocity, since the effects of flame stretch, instabilities and cellularity do affect the obtained velocity. In other words, reported hydrogen combustion velocities are not the same concept for all authors.

Laminar flame velocity can be only strictly defined for a one-dimensionally propagating, planar flame, without heat losses and in the absence of flow instabilities. In all experimental devices, stretch effects (due to flame curvature and its rate of change), and instabilities (both hydrodynamic and thermodiffusive) are present, apart from other effects such as heat losses. Both causes affect the flame velocity that can be measured directly or obtained by a means of an analysis procedure, as in the present paper. Corrections based on combustion theory can be introduced to account for these effects and try to obtain the laminar flame velocity, although frequently the published results do not consider them, which is a cause of the spread of data on the laminar values.

Stretch rate reduces experimental values of combustion velocity, which is important at small values of flame radius (and usually associated to combustion low pressures). On the other hand, flame development leads to big values of flame radius, with reduced stretch, but with an increased trend to instabilities, favoured by higher pressure values. In fact, most laminar flames at engine pressures and temperatures become cellular in nature due to instabilities. This means that the apparent quasi-laminar burning velocity is higher than the actual laminar velocity (as computed by assuming a smooth flame surface).

Other researchers obtain the combustion velocity based on an analytical, computational approach, by considering kinetic schemes. Assumptions can be made of adiabatic conditions, planar flame front, steady conditions and absence of instabilities, in order to compute the theoretical value of the laminar velocity, very difficult to achieve from experimental measurements. For that reason, it is not surprising that the trends of the purely kinetical results are different from the strictly experimental results without corrections.

From the comparison of burning velocities derived from flame speed measurements (with thermodynamic or optical-image analysis) and results predicted by computation of reaction kinetics, it can be seen that the burning velocities determined by measurements are in general higher than the values given by the kinetic schemes. This can be appreciated in Figure 14, since the results of three of the experimental methods considered (Ijima [21], Milton [35], present authors) have similar trends and values higher than the results of the kinetic methods. The results of these three experimental methods relative to burning velocity are affected by actual conditions of stretch and instabilities (including cellularity). The fourth experimental method (Verhelst et al. [37]) has the same trend, but with smaller values. A possible reason for this difference is that the first three methods are based on the analysis of registered pressure, while

the fourth is based on recording and treating flame images, providing different estimations of flame velocity. A more complete discussion can be found in Mayo [62].

Relative to the numerical methods (Verhelst et al. [36], Knop et al. [38], D'Errico et al. [39], Hu et al. [41], Gerke et al. [42], Verhelst et al. [43], Gottgens et al. [44], and Bougrine et al. [45]), based on the analysis of their particular assumptions, it can be said that not all of them strictly provide the value of the theoretical laminar flame velocity concept. In fact there is a strong dispersion even in the trends, especially at high temperatures (and associated compression pressures). Up to 550 K, most of the analytical values are between 50 and 60% of the experimentally obtained results, usually considered higher than the laminar theoretical concept.

As a summary, it can be said that, while kinetic models have interest to obtain the theoretical laminar velocity, results of experimental methods also have interest to obtain the values of apparent laminar velocity, i.e. the velocity that can be achieved in practical devices. In addition, for engine simulations, frequently a flame speed ratio (given by flow turbulence) is used to obtain the turbulent flame speed from the laminar flame velocity). This means that expressions such as the ones proposed by the authors in this paper are useful for engine simulation.

5. Conclusions

A methodology to obtain the burning velocity of gaseous fuel mixtures at pressure and temperature conditions similar to the ones found in spark ignition engines has been presented. The methodology has two parts: first obtaining the pressure during the combustion process of a quiescent homogenous mixture of fuel and oxidant in a constant volume combustion bomb, and second analysing the experimental pressure by means of a combustion model in order to obtain temperatures, flame front position and combustion velocity. This methodology has been validated with methane-air mixtures and later on it has been used to determine burning velocities of hydrogen-air mixtures.

Great care has been given to have a high repeatability of the method, as well as to establish the right range of validity of results, by, for instance, considering overlapping sets of combustion processes with enchainned initial conditions. However, this method does not allow direct observation of the flame front evolution, which means that it is more difficult to analyse aspects as the relationship between the stretch rate and the laminar burning velocity, or the study of the cellular structure of a flame at certain conditions of pressure and temperature.

By combining the results of experiments covering ranges of initial pressure and temperature, and fuel/air ratio, it is possible to obtain enough data to establish analytical correlations for the burning velocity of a given fuel as a function of the pressure, temperature of the unburned mixture and equivalence ratio.

In the case of methane/air mixtures, correlations have been obtained for purely laminar combustion velocity (excluding the cellular regime). There are different correlations for specific values of equivalence ratio and a general correlation for the range of values of equivalence ratio from 0.7 to 1.2 (Eq. 2 and Table 2, valid up to 0.7 MPa and 480 K). The validity of these correlations has been indirectly checked by comparing the burning velocity at ambient conditions (1 MPa and 300 K) with other published values, showing a good agreement.

In addition, the results for moderate pressures and temperatures have also been compared with the results of other authors.

Results for the burning velocity of hydrogen/air mixtures are also presented in the form of a correlation (Eq. 3, up to 1.6 MPa and 650 K) for stoichiometric conditions. A comparison of the proposed values with other published correlations has also been done. The proposed correlation provides values for the burning velocity that are in agreement with other obtained with similar experimental techniques, that in general include the effects of cellularity, since this appears even at moderate pressures. A discussion is included relative to the values provided by the straight experimental methods as compared to computational methods, which are aimed to obtain the laminar theoretical concept.

ACKNOWLEDGMENT

The authors of this work would like to thank the Spanish Ministry of Science and Innovation for the financial support of this research through the ENE 2012-34830 (with FEDER funds) and the Regional Government of Castile and Leon for funding the Excellence Research Group GR203.

ABBREVIATIONS AND NOMENCLATURE

A_f	Flame front area
C_c	Burning velocity
CVCB	Constant volume combustion bomb
h	Specific enthalpy
m	Mass
\dot{m}_b	Mass burning rate
p	Pressure
R_f	Flame front radius
RICE	Reciprocating internal combustion engines
SIE	Spark Ignition Engine
T	Temperature
V	Volume

Greek symbols

α	Temperature exponent in Equation 2
β	Pressure exponent in Equation 2
γ	Ratio of heat capacities
Φ	Fuel/air equivalence ratio
ρ	Density

Subscripts

0	Reference conditions
b	Burned
i	Initial
ub	Unburned

REFERENCES

- [1] F.N. Egolfopoulos, P. Cho, C.K. Law, Laminar flame speeds of methane-air mixtures under reduced and elevated pressures, *Combustion and Flame*, 76 (1989) 375-391.
- [2] A. Van Maaren, D.S. Thung, L.R.H. De Goey, Measurement of Flame Temperature and Adiabatic Burning Velocity of Methane/Air Mixtures, *Combustion Science and Technology*, 96 (1994) 327-344.
- [3] K.K. Kuo, *Principles of Combustion*, Wiley, 1986.
- [4] P. Clavin, Dynamic behavior of premixed flame fronts in laminar and turbulent flows, *Progress in Energy and Combustion Science*, 11 (1985) 1-59.
- [5] F.A. Williams, *Combustion Theory*, 1985.
- [6] F.N. Egolfopoulos, N. Hansen, Y. Ju, K. Kohse-Höinghaus, C.K. Law, F. Qi, Advances and challenges in laminar flame experiments and implications for combustion chemistry, *Progress in Energy and Combustion Science*, 43 (2014) 36-67.
- [7] B.H. Chao, F.N. Egolfopoulos, C.K. Law, Structure and propagation of premixed flame in nozzle-generated counterflow, *Combustion and Flame*, 109 (1997) 620-638.
- [8] Z. Zhao, A. Kazakov, F.L. Dryer, Measurements of dimethyl ether/air mixture burning velocities by using particle image velocimetry, *Combustion and Flame*, 139 (2004) 52-60.
- [9] F.N. Egolfopoulos, H. Zhang, Z. Zhang, Wall effects on the propagation and extinction of steady, strained, laminar premixed flames, *Combustion and Flame*, 109 (1997) 237-252.
- [10] C.K. Law, C.J. Sung, Structure, aerodynamics, and geometry of premixed flamelets, *Progress in Energy and Combustion Science*, 26 (2000) 459-505.
- [11] M. Mizomoto, H. Yoshida, Effects of Lewis number on the burning intensity of Bunsen flames, *Combustion and Flame*, 70 (1987) 47-60.
- [12] T.C. Wagner, C.R. Ferguson, Bunsen flame hydrodynamics, *Combustion and Flame*, 59 (1985) 267-272.
- [13] D. Bradley, Flame Propagation in a Tube: The Legacy of Henri Guenoche, *Combustion Science and Technology*, 158 (2000) 15-33.
- [14] H. Schneider, Measurement of turbulent burning velocities by means of the open tube method, *Journal of Loss Prevention in the Process Industries*, 19 (2006) 130-134.
- [15] A.E. Dahoe, Laminar burning velocities of hydrogen-air mixtures from closed vessel gas explosions, *Journal of Loss Prevention in the Process Industries*, 18 (2005) 152-166.
- [16] F. Tinaut Fluixá, B. Giménez Olavarría, D. Iglesias Hoyos, M. Lawes, Experimental Determination of the Burning Velocity of Mixtures of n-Heptane and Toluene in Engine-like Conditions, *Flow, Turbulence and Combustion*, 89 (2012) 183-213.
- [17] D. Bradley, R.A. Hicks, M. Lawes, C.G.W. Sheppard, R. Woolley, The Measurement of Laminar Burning Velocities and Markstein Numbers for Iso-octane-Air and Iso-octane-n-Heptane-Air Mixtures at Elevated Temperatures and Pressures in an Explosion Bomb, *Combustion and Flame*, 115 (1998) 126-144.
- [18] X.J. Gu, M.Z. Haq, M. Lawes, R. Woolley, Laminar burning velocity and Markstein lengths of methane-air mixtures, *Combustion and Flame*, 121 (2000) 41-58.
- [19] D.D. Agrawal, Experimental determination of burning velocity of methane-air mixtures in a constant volume vessel, *Combustion and Flame*, 42 (1981) 243-252.
- [20] A.E. Dahoe, L.P.H. de Goey, On the determination of the laminar burning velocity from closed vessel gas explosions, *Journal of Loss Prevention in the Process Industries*, 16 (2003) 457-478.
- [21] T. Iijima, T. Takeno, Effects of temperature and pressure on burning velocity, *Combustion and Flame*, 65 (1986) 35-43.

- [22] M. Metghalchi, J.C. Keck, Burning velocities of mixtures of air with methanol, isooctane, and indolene at high pressure and temperature, *Combustion and Flame*, 48 (1982) 191-210.
- [23] A. Lafuente, A Methodology for the diagnostic of the laminar velocity of gaseous fuel mixtures from the measurement of the pressure register in a constant volume combustion bomb, in, Vol. PhD Thesis, University of Valladolid, 2008.
- [24] M.I. Hassan, K.T. Aung, G.M. Faeth, Measured and predicted properties of laminar premixed methane/air flames at various pressures, *Combustion and Flame*, 115 (1998) 539-550.
- [25] L. Gillespie, M. Lawes, C. Sheppard, R. Woolley, Aspects of Laminar and Turbulent Burning Velocity Relevant to SI Engines, SAE Technical Paper, 2000-01-0192 (2000).
- [26] D. Bradley, C.G.W. Sheppard, R. Woolley, D.A. Greenhalgh, R.D. Lockett, The development and structure of flame instabilities and cellularity at low Markstein numbers in explosions, *Combustion and Flame*, 122 (2000) 195-209.
- [27] C.M. Vagelopoulos, F.N. Egolfopoulos, Direct experimental determination of laminar flame speeds, Symposium (International) on Combustion, 27 (1998) 513-519.
- [28] C.M. Vagelopoulos, F.N. Egolfopoulos, Laminar flame speeds and extinction strain rates of mixtures of carbon monoxide with hydrogen, methane, and air, Symposium (International) on Combustion, 25 (1994) 1317-1323.
- [29] K.J. Bosschaart, L.P.H. de Goey, The laminar burning velocity of flames propagating in mixtures of hydrocarbons and air measured with the heat flux method, *Combustion and Flame*, 136 (2004) 261-269.
- [30] 95/06364 Response to comment by S.C. Taylor and D.B. Smith on 'Laminar burning velocities and Markstein numbers of hydrocarbon/air flames', *Fuel and Energy Abstracts*, 36 (1995) 450.
- [31] R. Stone, A. Clarke, P. Beckwith, Correlations for the Laminar-Burning Velocity of Methane/Diluent/Air Mixtures Obtained in Free-Fall Experiments, *Combustion and Flame*, 114 (1998) 546-555.
- [32] M. Akram, P. Saxena, S. Kumar, Laminar Burning Velocity of Methane–Air Mixtures at Elevated Temperatures, *Energy & Fuels*, 27 (2013) 3460-3466.
- [33] R.T.E. Hermanns, A.A. Konnov, R.J.M. Bastiaans, L.P.H. de Goey, K. Lucka, H. Köhne, Effects of temperature and composition on the laminar burning velocity of CH₄ + H₂ + O₂ + N₂ flames, *Fuel*, 89 (2010) 114-121.
- [34] C. Tang, Z. Huang, C. Law, Determination, correlation, and mechanistic interpretation of effects of hydrogen addition on laminar flame speeds of hydrocarbon–air mixtures, *Proceedings of the combustion institute*, 33 (2011) 921-928.
- [35] B.E. Milton, J.C. Keck, Laminar burning velocities in stoichiometric hydrogen and hydrogen-hydrocarbon gas mixtures, *Combustion and Flame*, 58 (1984) 13-22.
- [36] A. Verhelst, A study of the combustion in hydrogen-fuelled internal combustion engines, in, University of Gent, 2005.
- [37] S. Verhelst, R. Sierens, A quasi-dimensional model for the power cycle of a hydrogen-fuelled ICE, *International Journal of Hydrogen Energy*, 32 (2007) 3545-3554.
- [38] V. Knop, A. Benkenida, S. Jay, O. Colin, Modelling of combustion and nitrogen oxide formation in hydrogen-fuelled internal combustion engines within a 3D CFD code, *International Journal of Hydrogen Energy*, 33 (2008) 5083-5097.
- [39] G. D'Errico, A. Onorati, S. Ellgas, 1D thermo-fluid dynamic modelling of an S.I. single-cylinder H₂ engine with cryogenic port injection, *International Journal of Hydrogen Energy*, 33 (2008) 5829-5841.
- [40] S. Verhelst, T. Wallner, Hydrogen-fueled internal combustion engines, *Progress in Energy and Combustion Science*, 35 (2009) 490-527.

- [41] E. Hu, Z. Huang, J. He, H. Miao, Experimental and numerical study on laminar burning velocities and flame instabilities of hydrogen–air mixtures at elevated pressures and temperatures, *International Journal of Hydrogen Energy*, 34 (2009) 8741-8755.
- [42] U. Gerke, K. Steurs, P. Rebecchi, K. Boulouchos, Derivation of burning velocities of premixed hydrogen/air flames at engine-relevant conditions using a single-cylinder compression machine with optical access, *International Journal of Hydrogen Energy*, 35 (2010) 2566-2577.
- [43] S. Verhelst, C. T'Joel, J. Vancoillie, J. Demuynck, A correlation for the laminar burning velocity for use in hydrogen spark ignition engine simulation, *International Journal of Hydrogen Energy*, 36 (2011) 957-974.
- [44] J. Göttgens, F. Mauss, N. Peters, Analytic approximations of burning velocities and flame thicknesses of lean hydrogen, methane, ethylene, ethane, acetylene, and propane flames, *Symposium (International) on Combustion*, 24 (1992) 129-135.
- [45] S. Bougrine, S. Richard, A. Nicolle, D. Veynante, Numerical study of laminar flame properties of diluted methane-hydrogen-air flames at high pressure and temperature using detailed chemistry, *International Journal of Hydrogen Energy*, 36 (2011) 12035-12047.
- [46] E. Hu, Z. Huang, J. He, C. Jin, J. Zheng, Experimental and numerical study on laminar burning characteristics of premixed methane–hydrogen–air flames, *International Journal of Hydrogen Energy*, 34 (2009) 4876-4888.
- [47] Z. Huang, Y. Zhang, K. Zeng, B. Liu, Q. Wang, D. Jiang, Measurements of laminar burning velocities for natural gas–hydrogen–air mixtures, *Combustion and Flame*, 146 (2006) 302-311.
- [48] D. Bradley, M. Lawes, R. Mumby, Burning velocity and Markstein length blending laws for methane/air and hydrogen/air blends, *Fuel*, 187 (2017) 268-275.
- [49] C. Ji, D. Wang, J. Yang, S. Wang, A comprehensive study of light hydrocarbon mechanisms performance in predicting methane/hydrogen/air laminar burning velocities, *International Journal of Hydrogen Energy*, 42 (2017) 17260-17274.
- [50] E.J.K. Nilsson, A. van Sprang, J. Larfeldt, A.A. Konnov, The comparative and combined effects of hydrogen addition on the laminar burning velocities of methane and its blends with ethane and propane, *Fuel*, 189 (2017) 369-376.
- [51] F.V. Tinaut, A. Melgar, B. Giménez, M. Reyes, Characterization of the combustion of biomass producer gas in a constant volume combustion bomb, *Fuel*, 89 (2010) 724-731.
- [52] A. Horrillo, Utilization of multi-zone models for the prediction of the pollutant emissions in the exhaust process in spark ignition engines, in, Vol. PhD Thesis, University of Valladolid, 1998.
- [53] J.B. Heywood, *Internal Combustion Engine Fundamentals*, New York, 1988.
- [54] H. Möhlenkamp, Zur Genauigkeit der Brenngesetzrechnung eines Dieselmotors mit nichtunterteiltem Brennraum, *MTZ*, 37 (1976) 8.
- [55] E. Hu, Z. Huang, J. He, J. Zheng, H. Miao, Measurements of laminar burning velocities and onset of cellular instabilities of methane–hydrogen–air flames at elevated pressures and temperatures, *International Journal of Hydrogen Energy*, 34 (2009) 5574-5584.
- [56] G.E. Andrews, D. Bradley, Determination of burning velocities: A critical review, *Combustion and Flame*, 18 (1972) 133-153.
- [57] P. Dirrenberger, H. Le Gall, R. Bounaceur, O. Herbinet, P.-A. Glaude, A. Konnov, F. Battin-Leclerc, Measurements of Laminar Flame Velocity for Components of Natural Gas, *Energy & Fuels*, 25 (2011) 3875-3884.
- [58] T. Tahtouh, F. Halter, C. Mounaïm-Rousselle, Measurement of laminar burning speeds and Markstein lengths using a novel methodology, *Combustion and Flame*, 156 (2009) 1735-1743.

- [59] F. Rahim, K. Eisazadeh Far, F. Parsinejad, R.J. Andrews, H. Metghalchi, A Thermodynamic Model to Calculate Burning Speed of Methane-Air- Diluent Mixtures, *International Journal of Thermodynamics*, 11 (2008).
- [60] D. Bradley, C. Sheppard, R. Woolley, Unstable explosion flames and acoustic oscillations, in: *18th Colloquium on the Dynamics of Explosions and Reactive Systems*, Seattle, USA, 2001.
- [61] C.K. Law, G. Jomaas, J.K. Bechtold, Cellular instabilities of expanding hydrogen/propane spherical flames at elevated pressures: theory and experiment, *Proceedings of the Combustion Institute*, 30 (2005) 159-167.
- [62] L. Mayo, An analysis of concepts and expressions for in-air laminar burning velocity of hydrogen and hydrogen-natural gas mixtures, in, *University of Valladolid*, 2016.

Table 1. Characteristics of the burning velocity results shown in Figure 8 for mixtures of methane and air.

Reference	Year	Method	p	T_{ub}
Vagelopoulos and Egolfopoulos [27]	1998	Stagnation flame with low stretch rates	1 atm	ambient
Vagelopoulos et al. [28]	1994	Counterflow burner	1 atm	ambient
Bosschaart and de Goey [29]	2002	Flat flame burner with heat flux control	atmospheric	295 K
Gu et al. [18]	2000	Recording of <i>flame radius</i> in the pre-pressure period in a CVCB	1 bar	300 K
Hassan et al. [23]	1998	Recording of <i>flame radius</i> in the pre-pressure period in a CVCB	1 bar	298 K
Aung et al. [30]	1995	Recording of <i>flame radius</i> in the pre-pressure period in a CVCB	1 atm	298 K
Stone et al. [31]	1998	Registration of pressure in a CVCB in free fall. Results presented as a correlation	1 bar	298 K
Present work		Registration of pressure in a CVCB, with thermodynamic analysis	1 bar	300 K
Akram et al. [32]	2013	<i>Diverging channel burner</i>	1 bar	298 K
Hermanns et al. [33]	2010	<i>Heat flux burner</i>	1 bar	298 K
Dirremberg et al. [57]	2011	<i>Heat flux method</i>	atmospheric	298 K
Tahtoug et al. [58]	2009	<i>Combustion bomb method</i>	atmospheric	298 K

Table 2. Coefficients and exponents of the laminar velocity correlation presented in Eq. 2, for different methane-air equivalence ratios for the ranges of pressure 0.1-0.7 MPa and temperature 320-480 K.

Φ	C_{c0}	α	β	R^2	$e_{standard}$
0.7	0.158	1.552	-0.262	0.967	0.0048
0.8	0.240	2.127	-0.403	0.994	0.0049
0.9	0.304	1.990	-0.364	0.992	0.0069
1.0	0.352	1.882	-0.352	0.995	0.0062
1.05	0.359	1.834	-0.340	0.994	0.0061
1.15	0.350	1.964	-0.399	0.995	0.0063
1.2	0.322	1.761	-0.343	0.985	0.0081
0.7-1.2	$0.355 - 1.650(\Phi-1.05)^2$	$1.894 + 0.202(\Phi-1)$	$-0.358 - 0.050(\Phi-1)$	0.992	0.0102

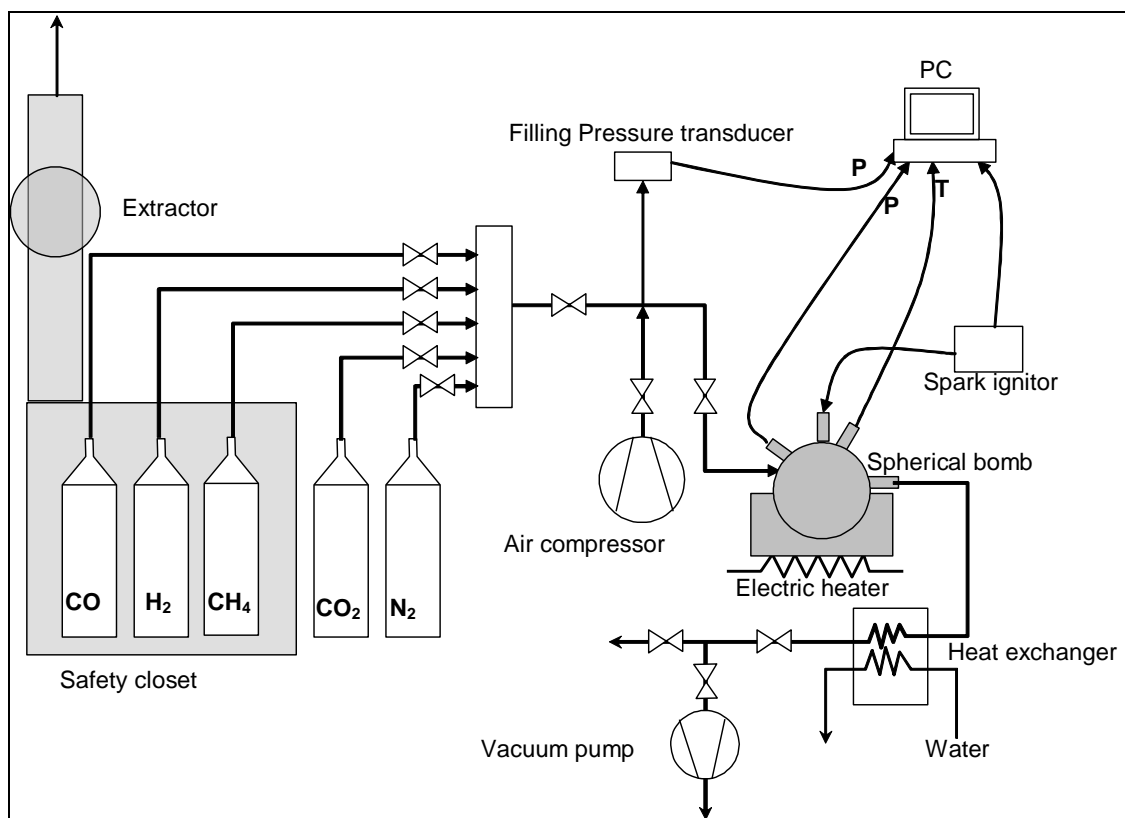


Figure 1. Schematics of the combustion bomb with the gas filling lines and data acquisition system.

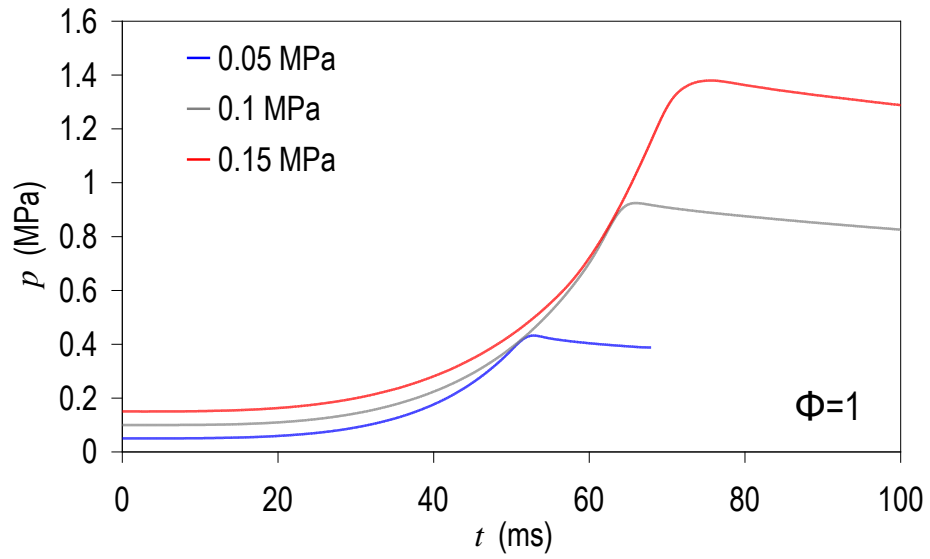


Figure 2. Temporal evolution of combustion pressure for a stoichiometric methane-air mixture with three initial pressures and 300K initial temperature.

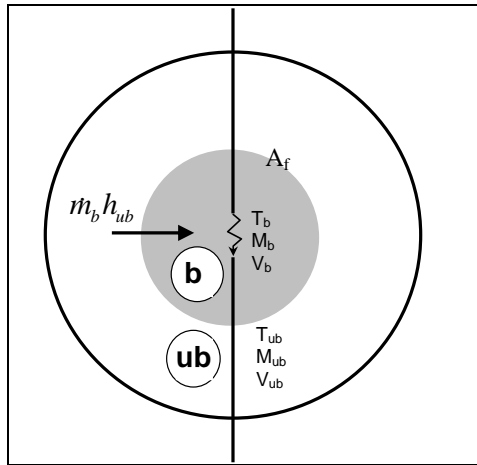


Figure 3. Outline of the two-zone combustion analysis model

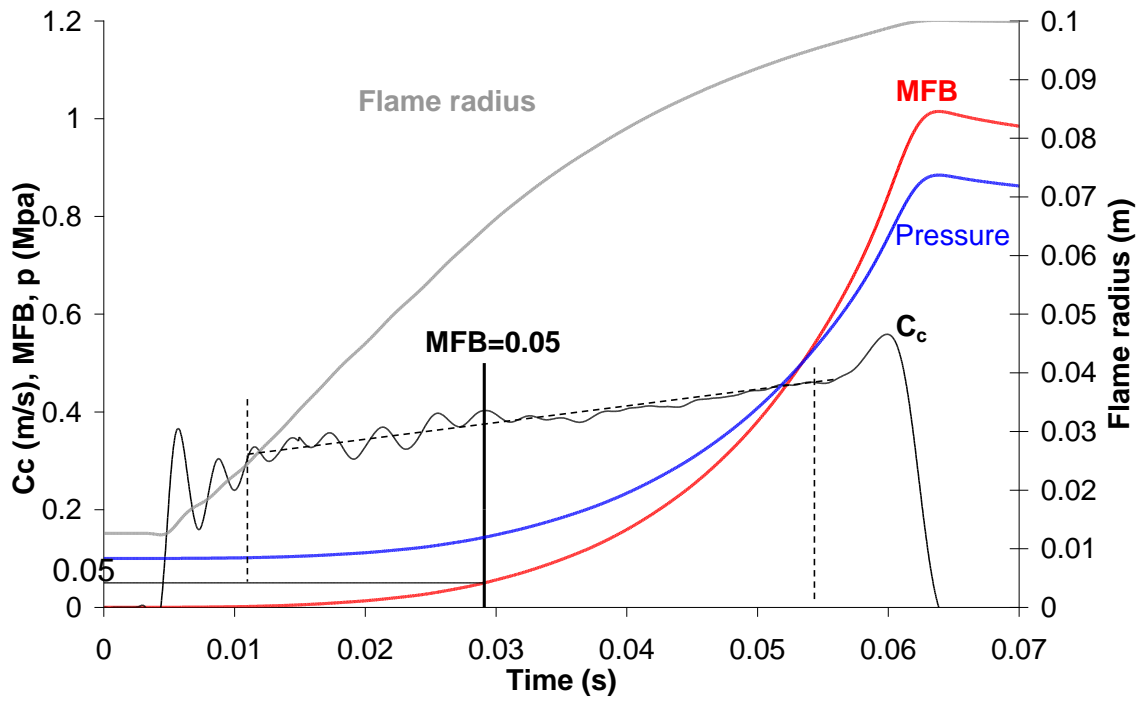


Figure 4. Burning velocity (C_c), mass fraction burned (MFB), pressure and flame front radius versus time.

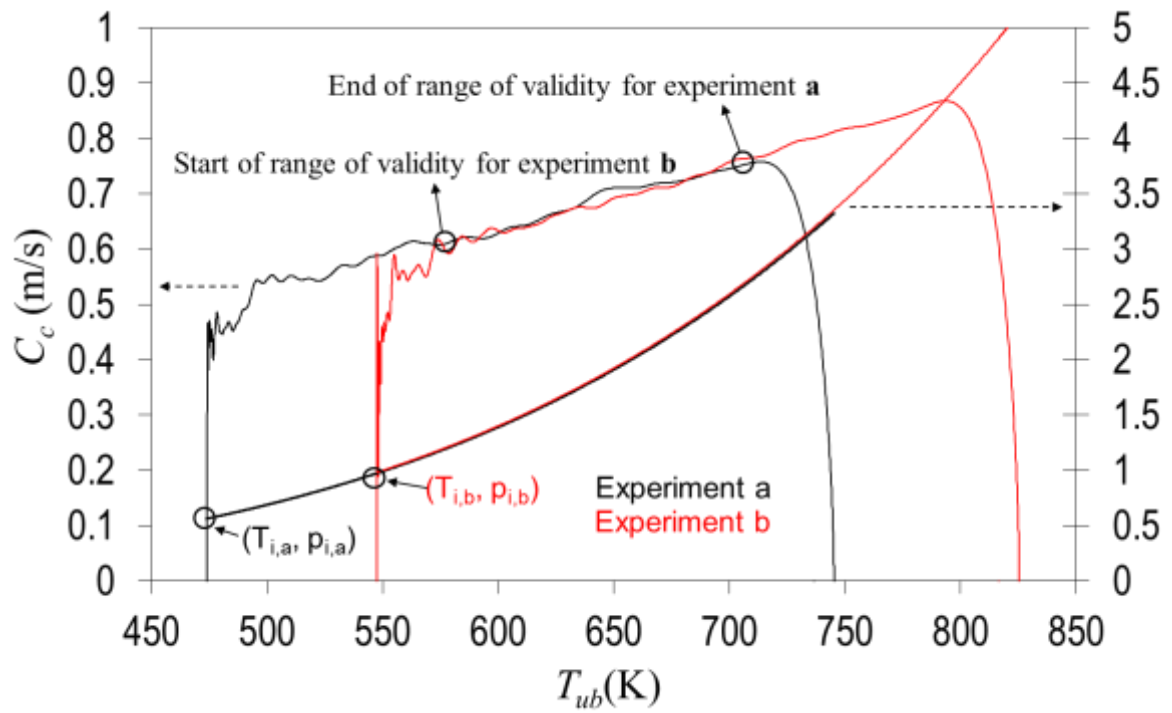


Figure 5. Overlapping of two burning velocity lines and the corresponding pressure lines for the same mixture but with different initial conditions (a-lower and b-higher).

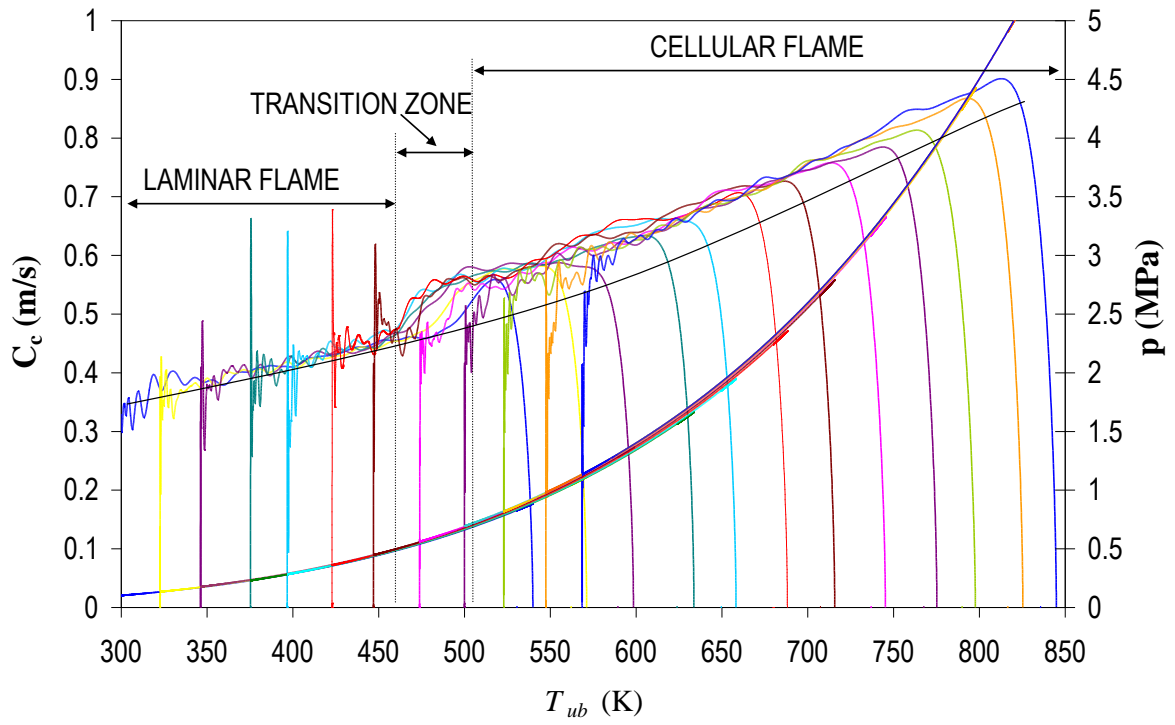


Figure 6. Overlapping plots of 12 combustion processes of a stoichiometric mixture of methane and air with increasingly higher initial conditions, starting at 298 K and 0.1 MPa (see text for explanation).

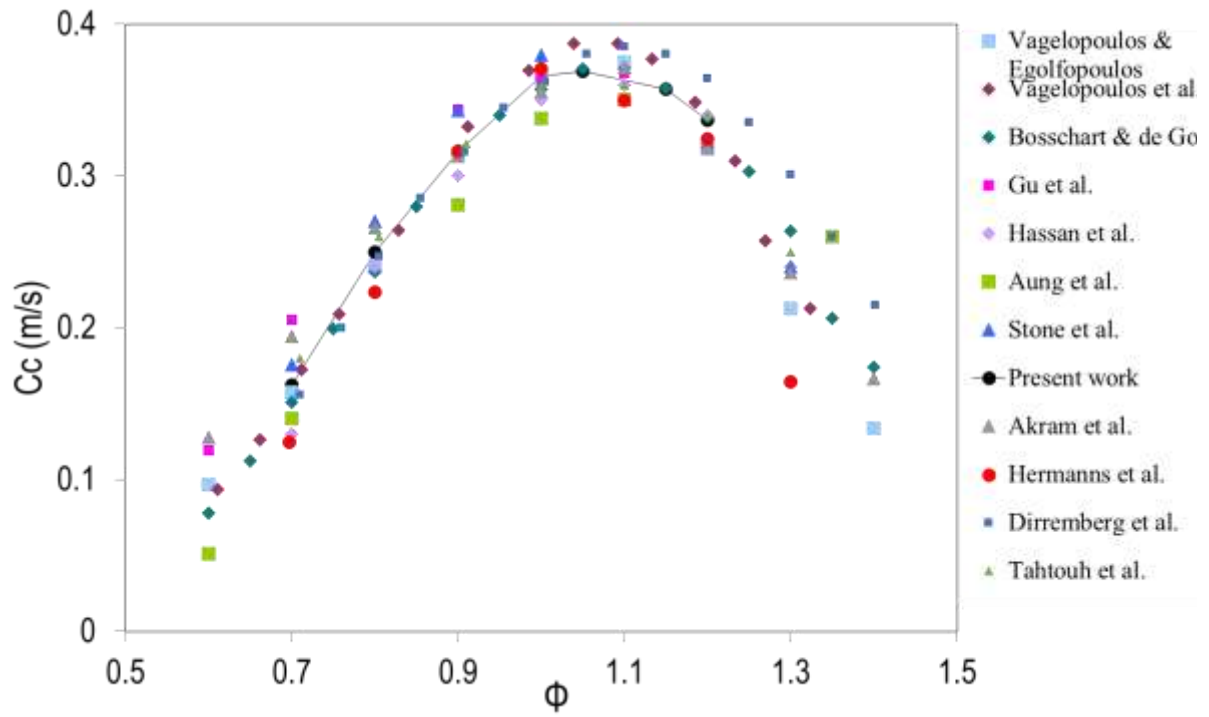


Figure 7. Comparison of the burning velocity results obtained by different authors (Table 1) for different fuel/air equivalence ratios of mixtures of methane and air at 0.1 MPa and 300

K.

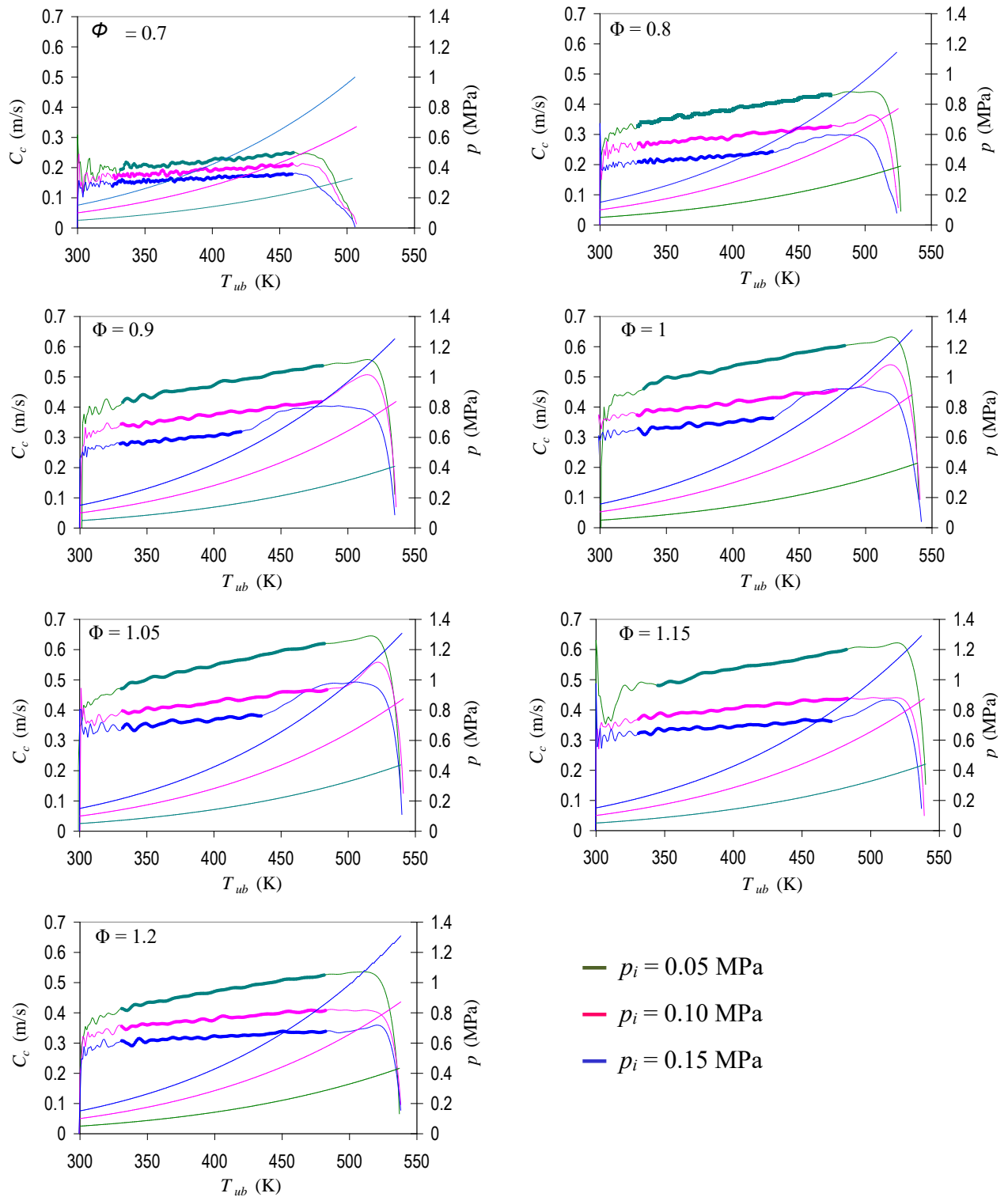


Figure 8. Evolution of the burning velocity and pressure versus the unburned temperature for the tested methane-air mixtures at 300 K initial temperature and three values of initial pressure. The ranges of laminar valid data in each velocity line are highlighted with a thick trace.

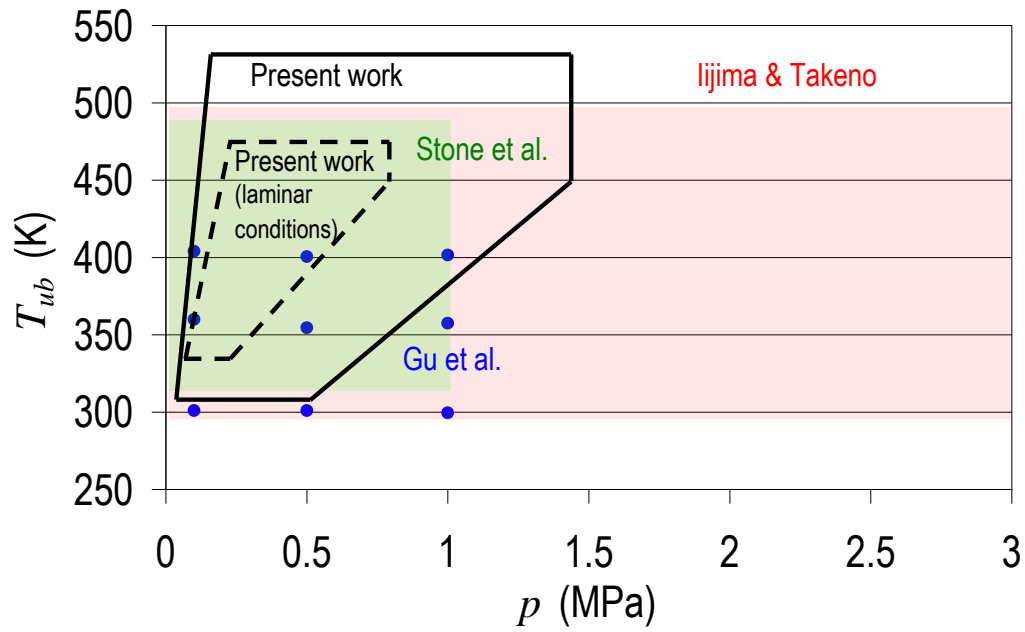


Figure 9. Thermal map with the range of validity of the correlations obtained in the present work (in broken lines, pure laminar conditions), compared with those covered by Iijima and Takeno^[21], Gu et al.^[18] and Stone et al.^[33] (that may include cellular conditions).

— Iijima and Takeno[21] — Gu et al.[18] — Stone et al.[33]
— Present work (Eq. 2) — Present work (experiments) — Pressure

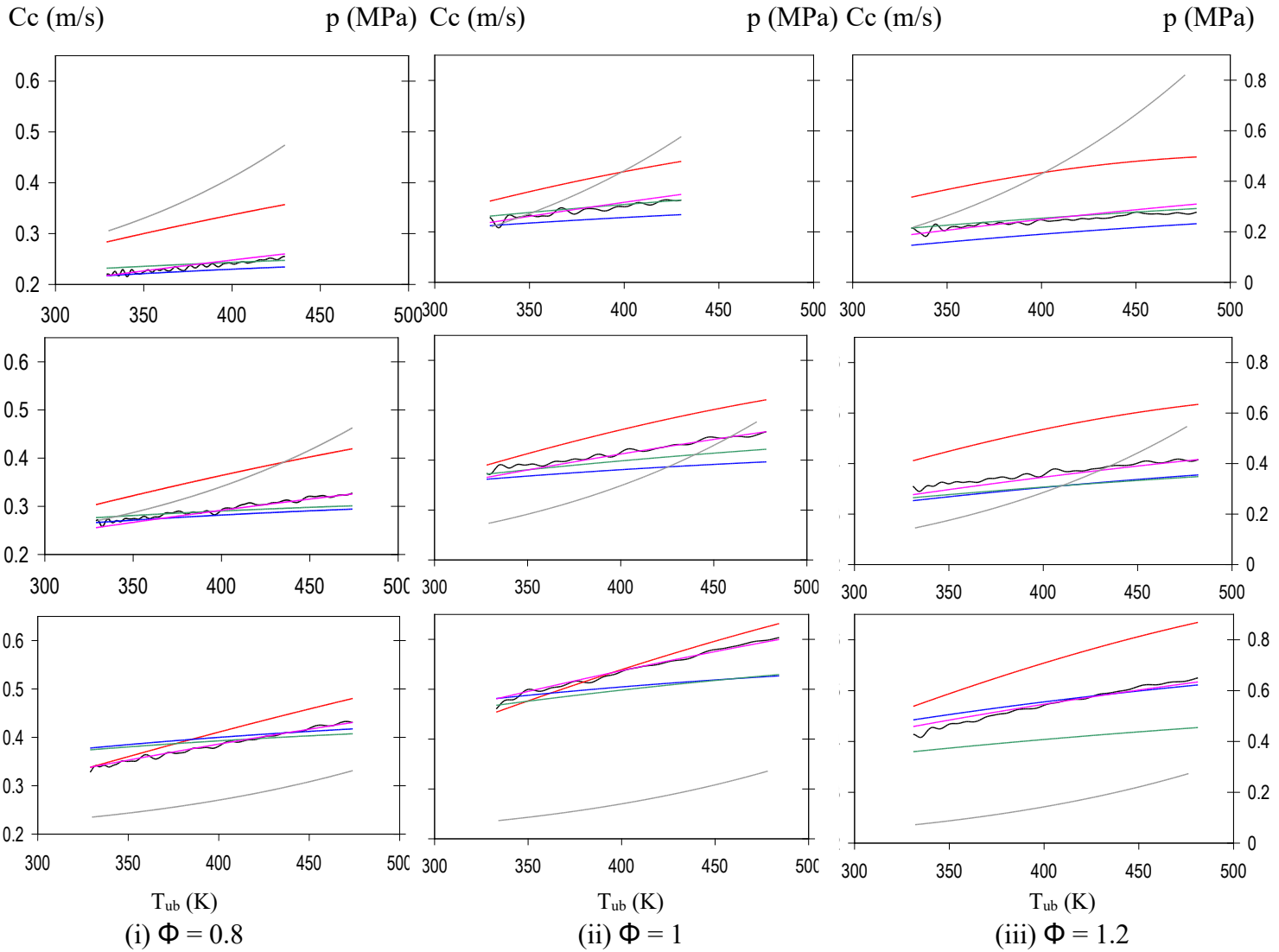


Figure 10. Comparison between the burning velocity values obtained experimentally (in black), proposed correlation (in fuchsia) and other authors' correlations in the purely laminar regimen, at moderate conditions, for a methane-air mixture as a function of unburned mixture temperature for different equivalence ratios. In each case, pressure increases with temperature as in an adiabatic compression, with initial values of 0.15 MPa (top), 0.10 MPa (middle) and 0.05 MPa (bottom).

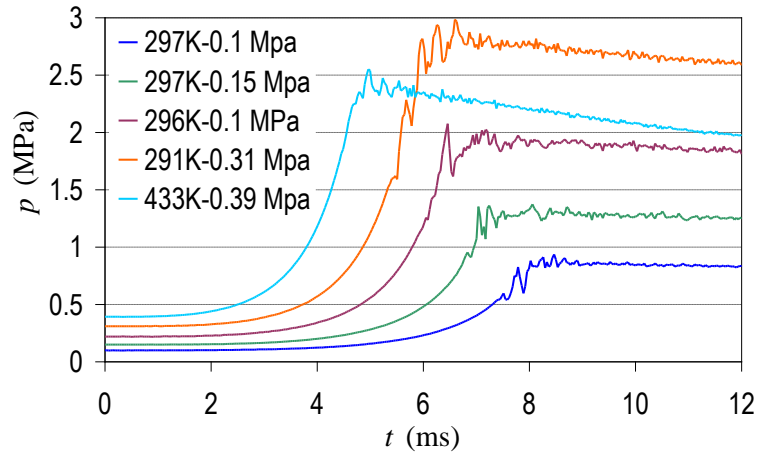


Figure 11. Pressure-time evolution plots for stoichiometric mixtures of hydrogen and air for different initial conditions of temperature and pressure (without filtering).

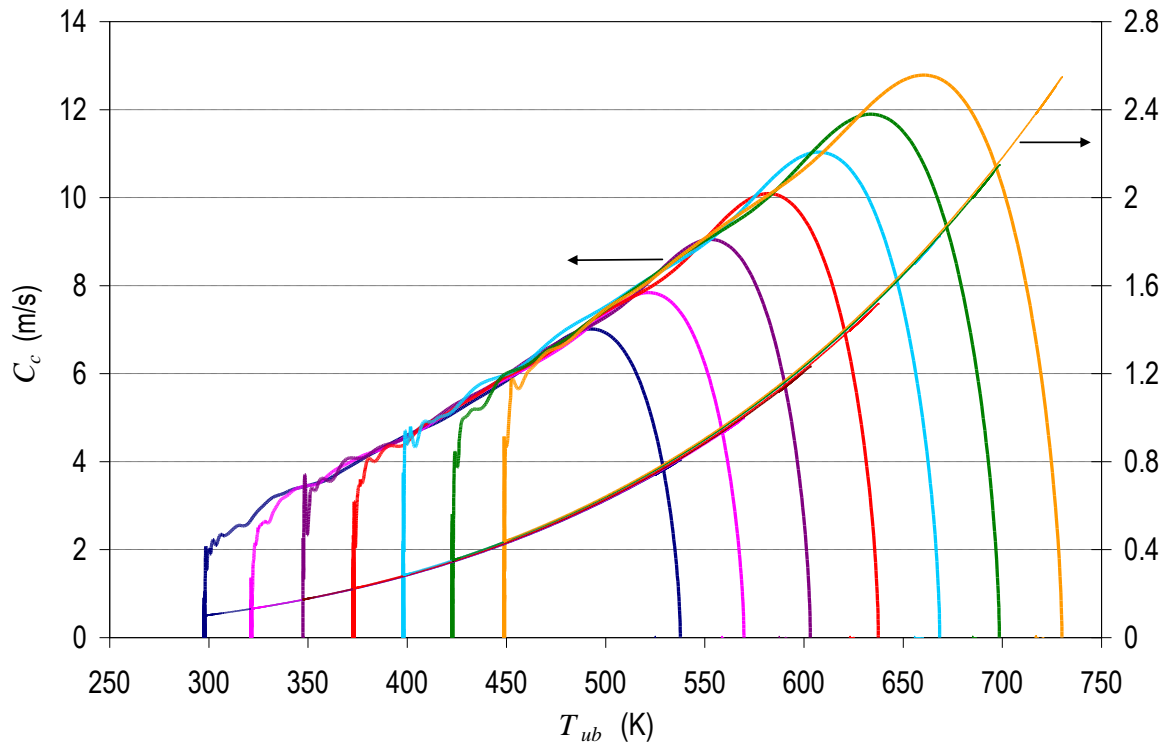


Figure 12. Overlapping curves of hydrogen/air mixtures at stoichiometric equivalence ratio. Evolution of the burning velocity (on the left axis) and pressure (on the right axis) versus the unburned temperature for seven experiments, the first with a 298 K temperature of and a 0.1 MPa pressure.

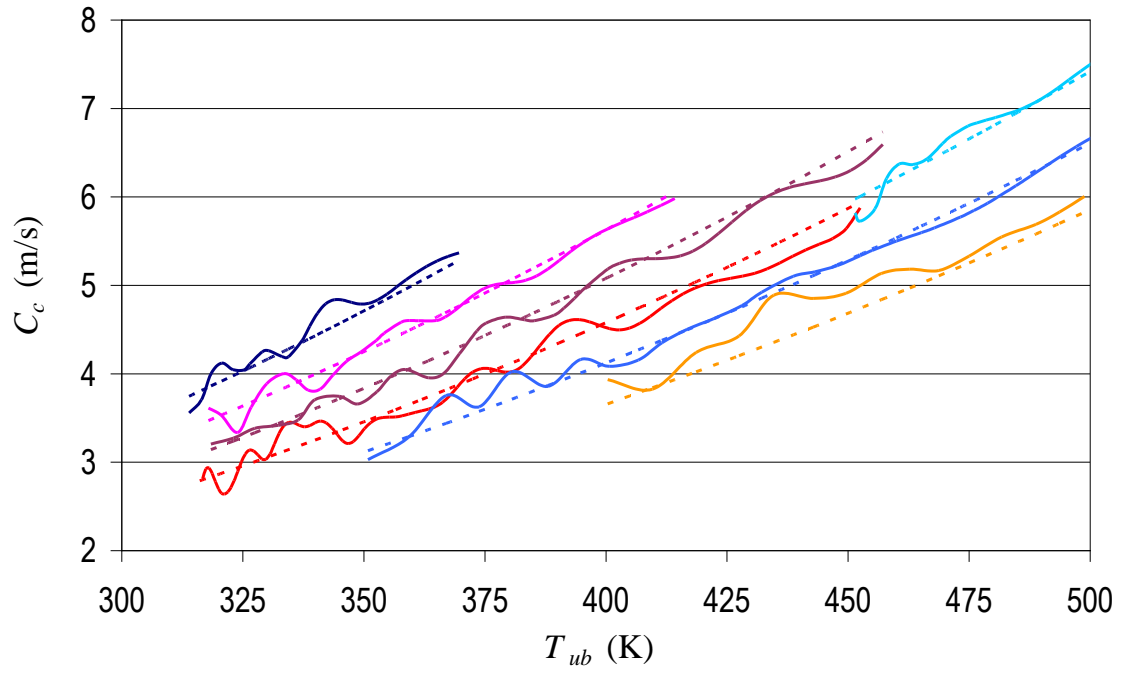


Figure 13. Comparison between experimental results (continuous lines) and values of Eq. 3 (broken lines) for experiments with increasing initial temperatures and related pressures.

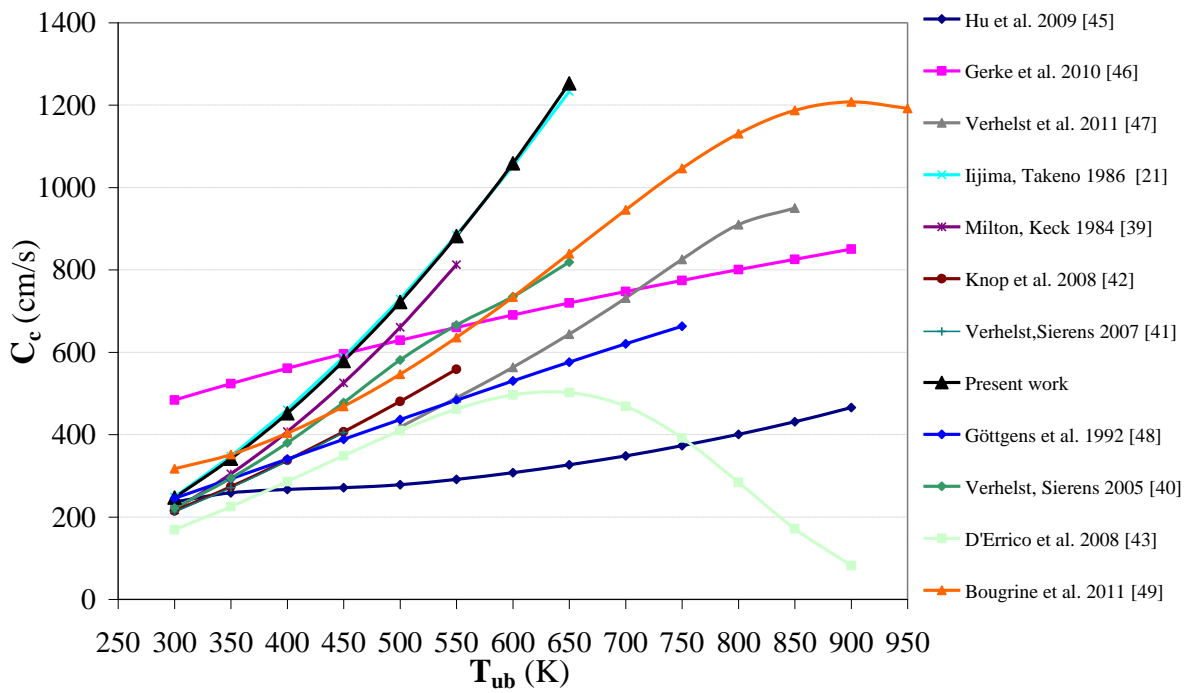


Figure 14. Comparison of the evolution of the burning velocity versus the unburned temperature with pressure growing according to an adiabatic compression, for hydrogen/air stoichiometric mixtures obtained by different authors’.

Highlights:

- Methodology to obtain the burning velocity of gaseous fuel mixtures
- Two zone two-zone thermodynamic combustion diagnosis model.
- Validation with methane laminar burning velocity.
- Burning velocity of hydrogen/air mixtures.